

Experimental Modeling of Central Axis and Jet-Ring Turbine Disk Cooling

Yong W. Kim* and Darryl E. Metzger†
Arizona State University, Tempe, Arizona 85287

The test facility, experimental methods, and summary results are presented from a study modeling turbine disk cooling with multiple impinging jets, such as employed on the Space Shuttle Main Engine oxygen turbopump. The study was designed to provide a comparison of detailed local convection heat transfer information obtained with a single center-supply of disk coolant, as opposed to the present flight configuration where disk coolant is supplied through an array of 19 radially outboard jets. Specially constructed turbine disk models were used in a program to evaluate possible benefits and tradeoffs of employing an alternate disk cooling scheme. The study involved the design, construction, and testing of two full-scale rotating model disks, one plane and smooth for baseline testing and the second contoured to the present flight configuration, together with the corresponding plane and contoured stators. Local heat transfer rates are determined from the color display of encapsulated liquid crystals coated on the disk in conjunction with use of a computer vision system. The test program was composed of a wide variety of disk speeds, flow rates, and geometrical configurations, including testing for the effects of bolt heads and hot gas entrainment into the disk cavity.

Nomenclature

c_p	= specific heat
h	= convection heat transfer coefficient
k	= thermal conductivity
Nu	= Nusselt number
Q	= total measured coolant volumetric flow rate
Q_p	= calculated free disk pumping flow
R	= flow ratio, Q/Q_p
Re_m	= flow Reynolds number, $Q/2\pi z\nu$
Re_r	= disk rotational Reynolds number, $\omega r^2/\nu$
r	= radial coordinate
r_i	= impingement radius
r_o	= disk radius
t	= temperature
t_i	= initial temperature
t_r	= reference temperature
t_s	= local surface temperature
z	= rotor-to-stator spacing
α	= thermal diffusivity
θ	= time
ν	= fluid kinematic viscosity
ρ	= fluid density
τ	= time step
ω	= angular velocity

Introduction

THE current flight configuration of the Space Shuttle Main Engine (SSME) HP oxidizer turbopump (HTOTP) employs 19 evenly spaced cooling jets impinging near its turbine disk outer radius. A detrimental dynamical behavior was identified, possibly associated with pressure excitation from the

multiple jets. As a result of this possibility, alternate cooling schemes that would employ coolant injection near the disk center were considered. Elimination of any dynamic problem would be eliminated with center impingement, but a question that arises with its employment is the degree of heat transfer capability that the coolant retains so far outboard of its supply location, and how that compares with the ability of the 19-jet configuration to keep the outer region of the disk cool.

This article summarizes the results of a program that involved the design, fabrication, and heat transfer testing of experimental models that simulate the cooled HPOTP turbine disk and its adjacent components, with both the 19-outboard jet array configuration and the single center supply configuration. Two disk/stator combinations were fabricated and used in the test program: 1) a contoured design that duplicates the actual SSME geometric details including disk contour, stator contour, and bolt patterns; and 2) a generic plane disk/plane stator design to provide baseline results. The test facility design also allows the introduction of a secondary flow simulating the availability of blade passages gases for entrainment into the disk cavity.

In general, convective heat transfer information on the faces of turbine disks is needed for the design of modern high-performance turbines in order to specify a cooling design that will insure acceptably low metal temperatures and temperature gradients, consistent with desired disk durability. Despite this need for detailed heat transfer information on rotating surfaces, such information has been acquired only slowly starting with, among others, the analysis of von Kármán¹ and the experiments of Cobb and Saunders² and Kreith et al.³ A concise review of literature addressing both the fluid mechanics and heat transfer aspects of the subject through 1982 is provided by Owen.⁴

Impingement of jets onto rotating disks, particularly onto turbine disks near the blade attachment region, has long been considered to be a potentially very effective method for turbine cooling, but one whose heat transfer mechanisms are not well understood. Some early measurements on actual cooled turbine hardware by Devyotov⁵ revealed anomalous results where heat transfer unexpectedly decreased with increasing disk speed. Subsequent laboratory studies with jets impinging on plane rotating surfaces (e.g., Refs. 6–9) have shown that a single isolated jet can easily be too weak to effectively penetrate the radially outward boundary-layer flow that is

Presented in part as Paper 91-0343 at the AIAA 29th Aerospace Sciences Meeting, Reno, NV, Jan. 6–9, 1991 and as Paper 92-0255 at the AIAA 30th Aerospace Sciences Meeting, Reno, NV, Jan. 7–10, 1992; received Feb. 10, 1993; revision received Sept. 13, 1993; accepted for publication Sept. 22, 1993. Copyright © 1993 by the American Institute of Aeronautics and Astronautics, Inc. All rights reserved.

*Visiting Assistant Professor, Department of Mechanical and Aerospace Engineering.

†Regents' Professor, Department of Mechanical and Aerospace Engineering. Associate Fellow AIAA.

always induced, or pumped, by the disk rotation. The interaction of an impinging jet onto a surface with boundary fluid pumped by the surface motion is quite different than the usual interaction of a jet with a crossflow. In the case of the moving surface, the jet encounters an ever stronger crossflow as it nears the surface, whereas in the more usual stationary surface case, the crossflow must reduce to zero at the surface. Some recently published data¹⁰ with three impinging jets suggest that the heat transfer effect of multiple jets may be predictable by superposition of single jet performance if the angular spacing between two neighboring jets is sufficiently large.

The current SSME HPOTP flight configuration has 19 evenly spaced cooling jets issuing from a 360-deg jet ring and impinging near the turbine disk outer radius. This jet configuration is duplicated in the present study, with local heat transfer measured with the jet ring as well as with center supply on two different disk/stator models. One model employs a generic plane disk and plane stator, while the other employs a contoured disk and stator which duplicate the current flight configurations.

The acquisition of heat transfer information for rotating disks has been slow and is still very incomplete because of the expense and complexity involved in making local heat transfer measurements on rotating surfaces. Conventionally, such measurements involve mounting expensive heat flux gauges, or spot heaters and thermocouples, on the disk surface, and transmitting electrical power and measurement signals from and to the rotating apparatus through slip rings. The heat transfer information acquired is usually in the form of averages over all or part of the disk. In the present study, very localized convection heat transfer rates are obtained by utilizing liquid crystal surface coatings together with a thermal transient test procedure.

In the present method, encapsulated liquid crystal coatings are sprayed directly onto the disk test surface and their response is observed and processed during the transient with automated computer vision and data acquisition systems. Local convection coefficients are calculated from the transient thermal response of the test surface, as determined by color indications from the thin coating. This technique applied to rotating surfaces has been developed over the past few years^{11,12} for situations where the disk is cooled by jets.

A significant advantage of the present test method concerns proper modeling of the thermal boundary conditions on all the wetted surfaces. Compared to other more conventional methods, the present experimental technique has a distinct feature that it yields useful local heat transfer coefficients on the surfaces of interest without having to impose unrealistic boundary conditions on others. This makes the present technique more suitable for disk cavity heat transfer research since the flowfields in the cavity often involve recirculating regions where the flow exchanges heat with both the stator and the rotor.

Experimental Apparatus and Procedures

Apparatus

Figure 1 shows a schematic of the experimental apparatus used in the present study. Rotational speeds up to 10,000 rpm are provided by a $\frac{1}{2}$ -hp induction motor driving an enclosed and sealed twin bearing quill through a flat belt. Continuously variable speed adjustment is provided by an autotransformer, and the disk speed is continuously monitored with a photoelectric pickup and a digital frequency counter.

The disk and shroud assembly is shown in Fig. 2 for two different test setups. The test disk for the smooth plane disk experiments is made of clear acrylic plastic having dimensions of 1.219- and 12.07-cm radius. The flight contoured disk is also made of clear acrylic plastic with a radius of 12.07 cm and has contours on one side that match the SSME configuration. The contoured disk thickness varies between 0.899–1.473 cm along the radius. Both test disks have 78 equally

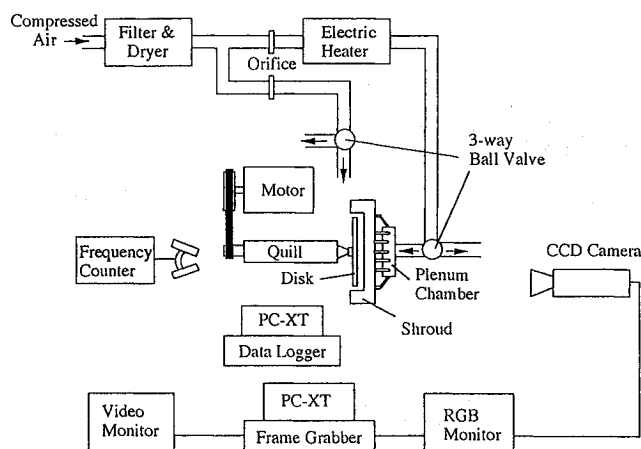


Fig. 1 Apparatus schematic.

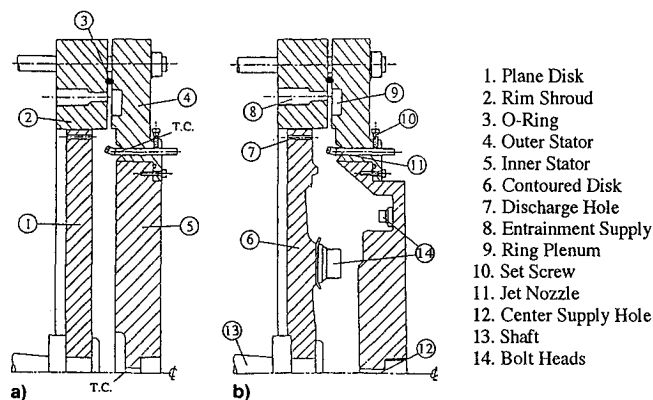


Fig. 2 Disk and stator assembly cross section: a) plane smooth and b) flight.

spaced 0.135-cm-diam holes at 11.68-cm radius, which simulate the coolant discharge flow passages.

The shroud assembly consists of three components made of acrylic plastic and aluminum. The front shroud piece is interchangeable, producing the disk and stator arrangements for the smooth plane disk and flight disk experiments shown in Fig. 2. The disk is maintained parallel to the stator with a shroud support assembly attached to the bearing housing, and the spacing is adjusted by moving the entire shroud assembly in the axial direction. The front shrouds have acrylic viewing windows (machined to match the shroud contour) which permits visual observations over the entire disk radius.

The 19-jet nozzles are made of brass, each having a nozzle tip with 0.132-cm exit diameter which is soldered to a 0.318-cm-i.d. tube. The nozzle tips are configured such that the jets they produce issue at an angle of 45 deg to the axial direction. The 19-jet supply nozzles are installed through 19 equally spaced positioning holes at 10.94-cm radius from the shroud center. Each nozzle is individually fixed with a set screw allowing two DOF for adjustment: axial translation and full 360-deg azimuthal rotation.

The impingement gap between disk and nozzle tip was maintained as 0.635 cm, and the disk-to-stator spacing was maintained as 1.27 cm for all smooth disk tests. The corresponding settings for the contoured configuration tests were 0.483 and 1.118 cm at the impingement radius. These settings are based on the SSME design configuration. The azimuthal angle for each nozzle was fixed at 13-deg radially outward for all tests, which also duplicates the SSME configuration.

All 19-jet supply nozzles are connected to a plenum chamber located near the front shroud through heat resistant plastic tubes. The plenum chamber serves as a flow distributor and is essentially a hollow disk with manifold holes configured such that heated air enters the chamber axially through one inlet port and exits radially in 19 equal parts distributed by

19 equally spaced holes on the rim. It was fabricated from a reinforced plastic (Lexan®) and is equipped with guard heaters to minimize heat losses. The guard heaters insure that the jet exit temperature remains high enough to produce the desired display of the disk liquid crystal surface coating. For tests with center supplied flow, the 19-jet plenum chamber is bypassed. In this case the heated air is directly injected axially through a 0.577-cm-diam hole located at the center of the front shroud.

In the present modeling of mainstream gas potentially entrained into the disk cavity, a controlled amount of secondary flow is supplied from another plenum chamber, with design similar to the jet supply plenum. Room temperature compressed air is divided into eight equal parts passing through the plenum chamber and delivered to the rear of the shroud rim by plastic tubes. Each jet first impinges onto a circumferential groove machined into the opposite facing shroud component and serving as a settling chamber. It is then introduced radially into the test section through a circumferential gap. The degree to which it is entrained into the disk cavity, as opposed to rapid turning and axially exit, can be at least partially indicated by its measured effect on the disk local heat transfer. With the present disk and shroud arrangement, all discharge flow is forced out through the 78 discharge holes near the disk rim and the disk-to-rim clearance gap which was measured to be 0.046 cm. The flow rates for all flows were measured using ASME standard orifices. The uniformity of the distribution of flow through the 19 jets was independently checked using a precision rotameter, and the 19 separate flows were found to be uniform within $\pm 5\%$.

The locations of thermocouples for jet temperature measurements are also indicated on Fig. 2. Five additional thermocouples were installed on the front shroud to monitor mid-point temperature variations at various locations within the wheel space. All thermocouples used were type K (Chromel-Alumel) with nominal wire diameter of 0.080 mm. The transient responses of the seven thermocouples monitoring jet and wheel space region temperatures were recorded through a data log unit (Fluke 2400 Intelligent Computer Front End) with a 0.4-s sampling interval for each thermocouple.

Measurement Procedures

The data reduction theory used in this investigation is well documented in Ref. 13, and the test procedures are similar to those described in Ref. 11. Therefore, only a brief overview will be given in this article. In the technique used, detailed local convection coefficients over the test region of interest are deduced from measurements of local transient wall temperature responses to the driving convective heating load based on established one-dimensional conduction theory.

The wall temperature response for one-dimensional heat conduction in a semi-infinite solid object to a step change in ambient fluid temperature is described by the following classical solution:

$$\frac{t_s - t_i}{t_r - t_i} = 1 - \exp\left(-\frac{h^2 \alpha \theta}{k^2}\right) \operatorname{erfc}\left(\frac{h\sqrt{\alpha \theta}}{k}\right) \quad (1)$$

With material properties known, h is inversely obtained from Eq. (1) with measurements of transient surface temperature response and fluid temperature t_r . In actual testing, a true step change in the fluid temperature is very difficult to achieve. However, the reference temperature can be measured as a function of time, and Eq. (1) is used as a fundamental solution to superpose the effect of a series of step changes in t_r using Duhamel's theorem, i.e.,

$$t_s - t_i = \sum_{j=1}^N U(\theta - \tau_j) \Delta t_r^j \quad (2)$$

where

$$U(\theta - \tau_j) = 1 - \exp\left(-\frac{h^2 \alpha (\theta - \tau_j)}{k^2}\right) \operatorname{erfc}\left(\frac{h\sqrt{\alpha (\theta - \tau_j)}}{k}\right)$$

For the acrylic plastic test surface material used, the depth of heating into the disk over the time duration needed to complete the test is less than the disk thickness. In addition, departure from one-dimensionality because of finite lateral conduction in the disk is not expected to have a significant effect on the local surface temperature response for the surface heat transfer gradients anticipated, as shown by Metzger and Larson¹³ and Vedula et al.¹⁴

In the present technique, the transient surface temperature information is provided by the application of a temperature indicating coating material, and a PC-based image processing system employing the frame grabber. The coating material used for this study is an encapsulated chiral nematic thermochromic liquid crystal (TLC), applied to the test surface using an airbrush. The TLC displays colors in response to temperature changes as a result of lattice reorientation of the crystal. When sprayed as a thin layer, the TLC is essentially clear and displays color with increasing temperature in sequence of red, green, blue, and back to clear. The nominal temperatures for the red, green, and blue displays of the crystal formulation used are 38.4, 39.8, and 43.5°C, respectively. The process is reversible and the calibration of temperature vs color remains unchanged for a large number of cycles under laboratory conditions. While all TLC coatings require a finite time for the necessary lattice rotations, Ireland and Jones¹⁵ have shown that microencapsulated chiral nematic coatings on the order of 10 mm thick require only a few milliseconds for this action. This time lag is negligible in comparison with the thermal transients of the present study.

A typical experimental run begins with heating laboratory compressed air to a desired temperature, while the test section is maintained at room temperature. A three-way ball diverter valve is used to route the heated air away from the test section until the air temperature reaches a preselected steady-state value indicated by a monitoring thermocouple in the diversion line. When steady state is nearly reached in the diversion line, the disk is brought to the desired test speed as rapidly as possible to minimize any possible temperature rise within the test region due to aerodynamic heating. Typically, the disk speed can be stabilized within 2 min with less than a 0.5°C increase in the recirculating air initially at room temperature. The heated air is then suddenly rerouted to the test section as the frame grabber and data log system for air temperature measurements are initiated simultaneously. For the tests with 19-jet supply, it is necessary to preheat the plenum chamber in order to improve the reference air temperature response, particularly at lower flow rates.

As the test surface is heated by the introduction of flow at elevated temperature, the local color information from the TLC coating is captured by a color video camera and digitized pixel-by-pixel with the frame grabber comparing to a preset threshold corresponding to the calibrated color intensity. The outcome of this image digitization process is a pixel time-temperature matrix covering the entire test region monitored by the video camera. This information, together with the transient reference temperature data, is sufficient for the high resolution determination of local convection coefficients using Eq. (2).

The preset threshold for a desired color is determined by calibrating the image processing system against a TLC-coated copper bar. The temperature response of the copper bar to a heat input is monitored by a thermocouple embedded in the bar. By varying the input threshold values, an optimum threshold and corresponding wall temperature can be acquired for given lighting conditions.

To minimize experimental uncertainties, the temperature of the supplied flow is chosen so that the color threshold is

not reached until sufficient time has elapsed after the start of flow (usually 10 s or more) to insure that the elapsed time can be determined accurately. Also, the flow temperature is chosen so that the elapsed time and corresponding penetration of the temperature pulse into the surface are small enough (usually less than 60 s) to insure that the test surface can be treated as semi-infinite as assumed in the data reduction. All of the results presented were obtained with threshold times satisfying these constraints, and the uncertainty in the measured convection coefficients is estimated to be $\pm 7\%$ by the methods of Kline and McClintock.¹⁶

Results and Discussion

Center Coolant Supply

Figures 3 and 4 show the measured local Nusselt numbers for the smooth plane disk with plane stator and single jet center coolant supply. Nu is defined as hr_0/k , where r_0 is the total disk radius, and the air thermal conductivity k is evaluated at a film temperature based on jet inlet and disk surface temperature measurements. With the local Nusselt number defined in this way, changes in the presented data represent solely the changes in h , with radius. In the present data reduction procedure, the heat transfer coefficient is based on the disk surface to jet inlet temperature difference.

Figure 3 shows results obtained for a Re_r of 3.14×10^5 and a Re_m of 2430. Re_r is defined as $\omega r_0/\nu$, where ω is the disk

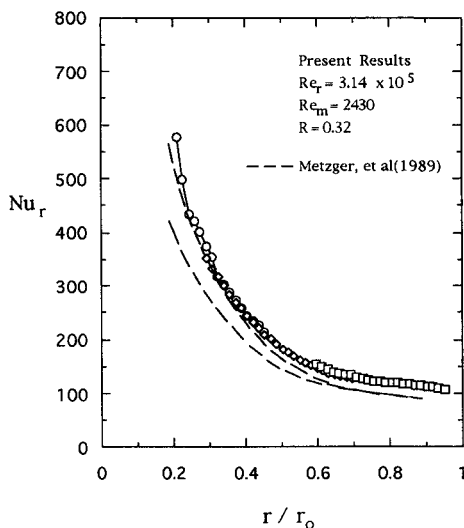


Fig. 3 Radial Nusselt number distribution, center supply, plane disk/stator.

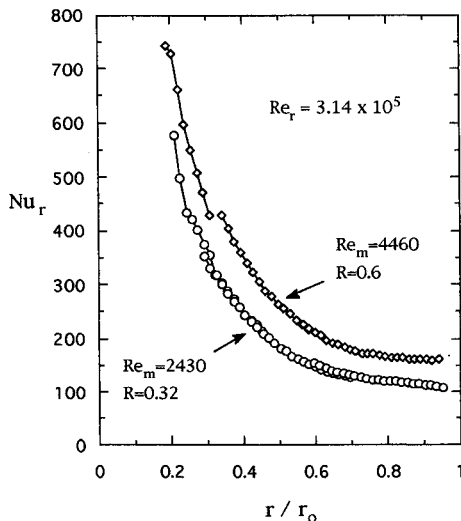


Fig. 4 Effect of Re_m on radial Nusselt number distribution, center supply, plane disk/stator.

rotational speed and ν is the kinematic viscosity. For convenience in later comparisons the radius r_i is used, where impingement takes place with the 19-jet cooling scheme, rather than r_0 . Re_m is defined as $Q/(2\pi z\nu)$, where Q is the supplied flow rate and z is the disk-to-stator spacing. Also indicated is R , the ratio of supplied flow rate Q , to the turbulent pumping flow rate Q_p , calculated from the von Karman's approximate solution based on the $1/7$ -th power law:

$$Q_p = 0.219r_i\nu Re_r^{0.8} \quad (3)$$

The pumping flow rate is evaluated at r_i . The presence of overlapping multiple lines of data results from the fact that a separate test needs to be conducted for each chosen radius range with a different jet supply temperature in order to minimize the experimental uncertainty associated with liquid crystal color transition times. In general, the agreement between overlapping data sets is very good, and lends confidence to the experimental method and data reduction procedure used. Further confidence is given by comparison with previous results obtained by Metzger et al.¹¹ for similar conditions, but with a different test rig. Their results are presented as dashed lines in Fig. 3 for the case of $Re_r = 2.71 \times 10^5$ with $Re_m = 1360$ (lower line) and 1900 (upper line).

It is noted that quite high heat transfer rates are measured near the disk center as a result of impingement and undiminished coolant temperature. However, these high heat transfer rates decrease rapidly with radius as the coolant loses its impingement character, and as the coolant-to-wall temperature difference decreases due to heat transfer to the disk and stator walls. Figure 4 shows the effect of increasing the flow Reynolds number on measured local Nusselt numbers. It is evident that local heat transfer rates increase with increasing coolant flow rate at all radial locations.

Figures 5 and 6 show the measured local Nusselt number distributions for the contoured flight disk and stator setup with single jet center coolant supply. Compared with the case of smooth plane disk and stator, data points are rather sparse, especially in the midradius region. This is the result of difficulties associated with viewing liquid crystal color responses through the Plexiglas® window which is contoured to match the stator contours. It was found impossible to illuminate the test surface uniformly over the entire radius, therefore, a separate calibration applicable to each region of interest was conducted and the data was reduced accordingly. The non-monotonic nature of data at the outer radii is thought to be the combined result of real variations in convection rates associated with the steps and ridges on the disk contours, along

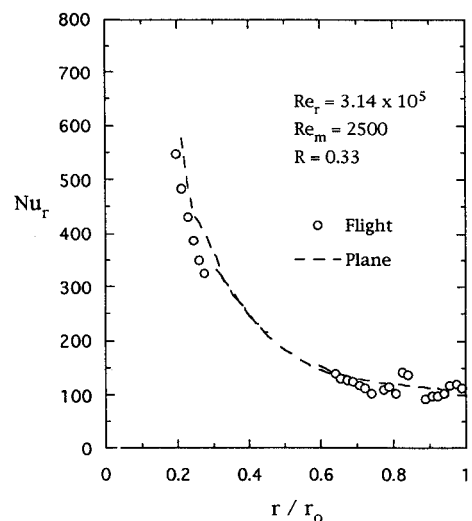


Fig. 5 Comparison between plane and flight disk/stator configurations, center supply.

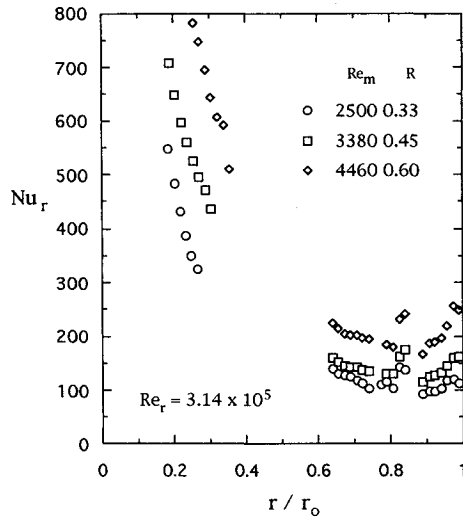


Fig. 6 Effect of Re_m on radial Nusselt number distributions, center supply, flight disk/stator, $Re_r = 3.14 \times 10^5$.

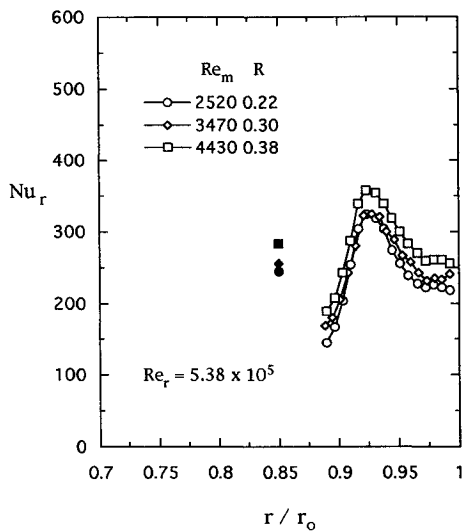


Fig. 7 Effect of Re_m on radial Nusselt number distributions, jet-ring supply, flight disk/stator.

with apparent difficulties with picking up color responses from sharply varying contoured surfaces.

Figure 5 shows the Nusselt number distributions obtained for $Re_r = 3.14 \times 10^5$ and $Re_m = 2500$. Shown as a dashed line on the figure is the data from the previous plane disk and stator results for matching conditions. The good agreement found in two sets of data confirms the result of a previous study by Metzger et al.⁷ that showed little effect of disk shape on heat transfer. Figure 6 shows the results of a parametric study in which the effect of flow Reynolds number on measured heat transfer rates is considered for a fixed rotational Reynolds number. The results display similar radial Nusselt number variations as for the plane disk cases, indicating that heat transfer rate increases with increasing flow Reynolds number.

19-Jet Ring Coolant Supply

Figure 7 shows the measured Nusselt number distributions with 19-jet ring coolant supply for the flight disk and stator configuration. The Nusselt number is defined the same as in the case of center supply. The heat transfer coefficient in this case is based on the air temperature measured at the nozzle inlet in one of the 19 equally spaced jet supply tubes and the disk surface temperature difference. The data summarize the results obtained for different jet flow rates with Re_r fixed at 5.38×10^5 . In general, the measured heat transfer monoton-

ically increases with increasing flow Reynolds number as indicated by the arithmetically averaged values, plotted as solid symbols at $r/r_0 = 0.85$. It is noted, however, that the dependence of local heat transfer rates on the value of Re_m is found to be relatively weak. For instance, a reduction in coolant flow rate of nearly 50% (as indicated by the parameter R) results in only about a 15% decrease in measured Nusselt number averaged over the effective radial position, whereas the data for the center supply case shown in Fig. 6 suggest a higher sensitivity for the same amount of percentage reduction in coolant flow rate.

It is noted that for the 19-jet ring supply the flow rate from each individual jet is less than 2% of the calculated disk pumping flow. Nevertheless, the measured heat transfer levels indicate that the 19 jets are surprisingly effective in providing cooling. Previous measurements by Metzger and Grochowsky,⁶ and subsequently by Metzger et al.,⁷ showed that jet impingement cooling on a rotating disk is ineffective until the jet flow rate reaches the order of 10% of the calculated disk pumping flow. However, this conclusion is based on the results obtained with one, to at most three, jets impinging on free disks with no shrouds, and therefore, a direct application of their findings in interpreting the present data is questionable. One plausible explanation for the high heat transfer rates measured in the present study is that the 19 jets spaced relatively close tend to protect each other from the crossflow, enabling each downstream jet to effectively penetrate the induced wall flow boundary layer.

Comparison Between Center and 19-Jet Ring Coolant Supply Schemes

In order to investigate the relative merits of the two disk cooling schemes under consideration, data sets available for comparison obtained with the flight disk and stator configuration are plotted in Figs. 8–10. The solid symbol plotted at $r/r_0 = 0.85$ in each figure represents the arithmetic mean of the local Nusselt numbers obtained for the 19-jet array cooling scheme. For all three jet ring flow rates tested, the peak values of convection coefficient obtained with impingement from the 19 jets are greater than the coefficients associated with the same flow rate supplied at a single center location. However, it is apparent that, for the three data sets obtained thus far, the difference between the impingement and center-supply coefficients decreases with increasing Re_m . In fact, at the highest value of Re_m , with $R = 0.38$, the peak and mean Nusselt numbers obtained with the 19-jet ring show no advantage over the outer 10% of the disk radius compared with the data obtained with the flow supplied at the disk center. Such a trend is apparently due to the relative lack of dependence of

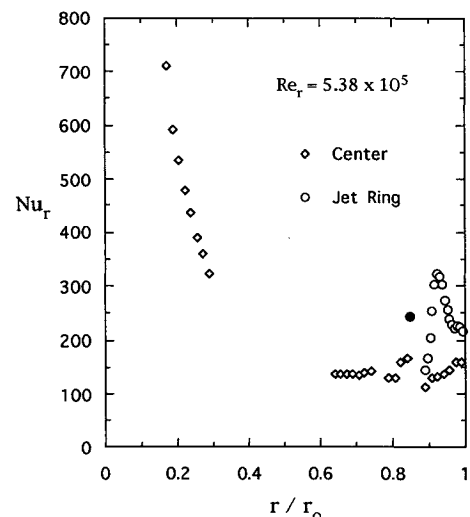


Fig. 8 Comparison between center and jet-ring supply, flight disk/stator, $Re_m = 2470$ – 2540 , $R = 0.21$ – 0.22 .

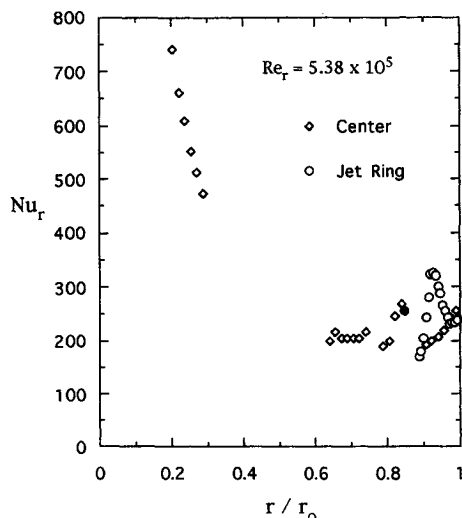


Fig. 9 Comparison between center and jet-ring supply, flight disk/stator, $Re_m = 3460$ – 3470 , $R = 0.30$.

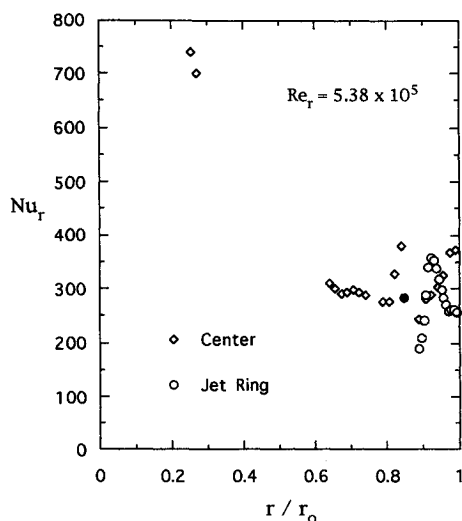


Fig. 10 Comparison between center and jet-ring supply, flight disk/stator, $Re_m = 4430$ – 4460 , $R = 0.38$ – 0.39 .

the 19-jet array data on Re_m . Combined with more significant dependence for the case of center supply, it acts to create a variation of relative cooling performance of these two coolant supply schemes with the flow Reynolds number. It is clear that more results are needed before a firm conclusion can be reached on the relative merits of the two coolant supply schemes.

Effect of Entrainment Flow

Figure 11 shows, for the 19-jet array supply, the measured effects on disk heat transfer of introducing a controlled amount of secondary flow which simulates an entrainment flow from the blade passage to the disk cavity region. This flow is supplied through a gap in the outer rim shroud at room temperature. In the present experimental method, the disk and shroud are initially at room condition and the coolant flow is suddenly applied at elevated temperature. The presence of a secondary flow maintained at room temperature near the test surface will effectively reduce the local wall-to-fluid temperature difference and will tend to drive the surface heat transfer in a direction opposing that of the coolant jets. Thus, if the entrainment flow is significantly intruding into the disk cavity, its presence will be evident through a measured decrease in local disk heat transfer rates.

For a given combination of Re_m and Re_r , two values of simulated entrainment flow rates were investigated: nominally, 6 and 10% of the calculated turbulent pumping flow

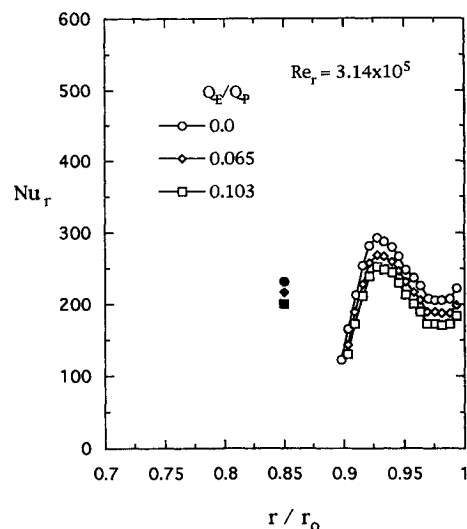


Fig. 11 Effect of simulated entrainment on radial Nusselt number distributions, plane disk/stator, $Re_m = 2530$, $R = 0.34$.

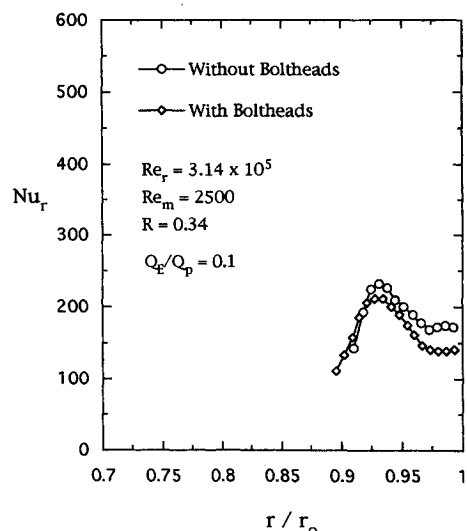


Fig. 12 Effect of bolt heads on radial Nusselt number distribution, with simulated entrainment.

based on the total disk radius. It is immediately apparent that the presence of the simulated entrainment flow is felt on the disk surface as indicated by the decreases in local and averaged (plotted as solid symbols) Nusselt numbers. The effects are observed more strongly as the amount of entrainment flow increases. Nevertheless, the resulting degradations in heat transfer are relatively small, and indicate that the jets are still quite effective in cooling the local region of the disk near their impingement radius. It should be emphasized that these results in Fig. 11 only serve to qualitatively indicate the presence of a heat transfer effect from the entrainment flow, and that they are insufficient to fully characterize the effect of entrainment flow on heat transfer rates. In general, the coolant jet and entrainment flow temperatures will be quite different, and together with the disk surface temperature, constitute a three-temperature convection situation where information on both convection coefficient and another parameter (usually termed effectiveness) are necessary to completely describe the heat transfer phenomenon, similar to the situation encountered with film-cooling injections.

Effect of Bolt Heads

Finally, Fig. 12 shows the measured effect, on local heat transfer near the impingement radius, of the presence of simulated bolt heads on the disk surface for a single combination

of Re_m , Re_s , and entrainment flow percentage. The measured local Nusselt number values obtained with the bolt heads in place are generally slightly lower than those measured without bolt heads. This trend is plausibly explained by the generation of a larger pumped flow with the bolts in place, which then interacts more forcibly with the impingement flow to reduce the penetration of the jets to the disk surface, although the data base is obviously not large enough to support any but the most tentative speculations. Nevertheless, even though the effects are small in these two instances, the effect is in the direction of decreased cooling capacity of the jet flow, and deserves to be investigated over a much wider range of conditions.

Summary and Conclusions

A full-scale contoured model of the SSME HPOTP turbine disk and stator has been designed and fabricated together with a similar generic version with plane and smooth disk and stator faces. The disks are designed for acquisition of detailed local convection heat transfer coefficient distributions using thin coatings of encapsulated liquid crystals. Transient thermal testing, together with the use of a computer vision data acquisition system to track the surface temperature response through the color display of the liquid crystals, has been successfully employed to acquire convection heat transfer information from both the plane and contoured rotating disks with two different coolant supply schemes. Based on the results presented, the following conclusions can be made:

- 1) Except for minor variations, the convection coefficients for the contoured disk and stator configuration are very similar to those for the plane disk and stator, both in magnitude and distribution. This observation concurs with the very limited prior information on the independent effect of disk shape.
- 2) For coolant supplied from the center of the disk cavity, the local heat transfer rates decrease monotonically from center to disk rim along the disk face.
- 3) For coolant supplied to the disk face from a jet ring near the disk outer radius, the location of significant coefficient magnitudes is restricted to the outer radius region, but their peak values are higher than those obtained with the center coolant supply, at least for the tests conducted thus far. However, the difference in the local heat transfer performance between two coolant supply schemes tends to decrease with increasing coolant flow rate for a fixed rotational Reynolds number.
- 4) For the present jet ring, the measured heat transfer effect of the 19 jets is more significant than found in previous studies, despite the fact that the flow rate from each individual jet is no more than 2% of the calculated disk pumping flow. It is believed that the combination of closely spaced jets around the complete circumference, and the presence of a closely spaced stator, act to improve jet penetration through the pumped boundary layer to the moving surface.
- 5) Because of the limited testing completed, any general conclusions regarding the relative merits of one coolant supply scheme over the other are premature and await further testing.
- 6) Although the presence of simulated entrainment acts to reduce the cooling rates for a given jet flow and disk speed, it does not appear to cause a major degradation in the jet ring cooling performance, at least over the parameter ranges covered in this study.
- 7) It is observed that bolt head simulations generally lower the overall cooling capability of the jet ring for a given test condition. Although the effect is small, such a trend deserves further studies at a wider range of parameters.

Acknowledgments

This work was supported by funds provided by NASA Marshall SFC through the Rocketdyne Division of Rockwell International Corporation, Canoga Park, California. Y. W. Kim wishes to express his deep sorrow for the untimely death of his mentor, D. E. Metzger, on August 1, 1993.

References

- ¹Von Kármán, T., "Über Laminare und Turbulente Reibung," *Zeitschrift fuer Angewandte Mathematik und Mechanik*, Vol. 1, 1921, p. 233.
- ²Cobb, E. C., and Saunders, O. A., "Heat Transfer from a Rotating Disk," *Proceedings of the Royal Society, London, Section A*, 236, 1956, p. 343.
- ³Kreith, F., Taylor, J. H., and Chong, J. P., "Heat and Mass Transfer from a Rotating Disk," *Journal of Heat Transfer, Transactions of the American Society of Mechanical Engineers*, Vol. 81, May 1959, pp. 95–105.
- ⁴Owen, J. M., "Fluid Flow and Heat Transfer in Rotating Disc Systems," *Heat and Mass Transfer in Rotating Machinery*, edited by D. E. Metzger and N. H. Afgan, Hemisphere, Washington, DC, 1984, pp. 81–103.
- ⁵Devaytov, V. I., "Investigation of Heat Transfer for Two Versions of Turbine Disk Cooling," *Aviatsionnaya Tekhnika*, Vol. 8, No. 2, 1965, pp. 56–64.
- ⁶Metzger, D. E., and Grochowsky, L. D., "Heat Transfer Between an Impinging Jet and a Rotating Disk," *Journal of Heat Transfer, Transactions of the American Society of Mechanical Engineers*, Vol. 99, Nov. 1977, pp. 663–667.
- ⁷Metzger, D. E., Mathis, W. J., and Grochowsky, L. D., "Jet Cooling at the Rim of a Rotating Disk," *Journal of Engineering for Power, Transactions of the American Society of Mechanical Engineers*, Vol. 101, Jan. 1979, pp. 68–72.
- ⁸Bogdan, Z., "Cooling of a Rotating Disk by Means of an Impinging Jet," *Proceedings of the 7th International Heat Transfer Conference*, Vol. 3, 1982, pp. 333–336.
- ⁹Popiel, C. O., and Boguslawski, L., "Local Heat Transfer from a Rotating Disk in an Impinging Round Jet," *Journal of Heat Transfer, Transactions of the American Society of Mechanical Engineers*, Vol. 108, May 1986, pp. 357–364.
- ¹⁰Metzger, D. E., and Partipilo, V., "Single and Multiple Jet Impingement Heat Transfer on Rotating Disks," AIAA Paper 89-0174, Jan. 1989.
- ¹¹Metzger, D. E., Bunker, R. S., and Bosch, G., "Transient Liquid Crystal Measurements of Local Heat Transfer on a Rotating Disk with Jet Impingement," *Journal of Turbomachinery, Transactions of the American Society of Mechanical Engineers*, Vol. 113, Jan. 1991, pp. 52–59.
- ¹²Bunker, R. S., Metzger, D. E., and Wittig, S., "Local Heat Transfer in Turbine Disk-Cavities, Part I: Rotor and Stator Cooling with Hub Injection of Coolant," *Journal of Turbomachinery, Transactions of the American Society of Mechanical Engineers*, Vol. 114, Jan. 1992, pp. 211–220.
- ¹³Metzger, D. E., and Larson, D. E., "Use of Fusion Point Surface Coatings for Local Convection Heat Transfer Measurements in Rectangular Channel Flows with 90-Degree Turns," *Journal of Heat Transfer, Transactions of the American Society of Mechanical Engineers*, Vol. 108, Feb. 1986, pp. 48–54.
- ¹⁴Vedula, R. P., Bickford, W., and Metzger, D. E., "Effects of Lateral and Anisotropic Conduction on Determination of Local Convection Heat Transfer Characteristics with Transient Tests and Surface Coatings," *Collected Papers in Heat Transfer*, American Society of Mechanical Engineers WAM HTD-Vol. 104, 1988, pp. 21–27.
- ¹⁵Ireland, P. T., and Jones, T. V., "The Response Time of a Surface Thermometer Employing Encapsulated Thermochromic Liquid Crystals," *Journal of Physics E: Scientific Instruments*, Vol. 20, Oct. 1987, pp. 1195–1199.
- ¹⁶Kline, S. J., and McClintock, F. A., "Describing Uncertainties in Single Sample Experiments," *Mechanical Engineering*, Vol. 75, Jan. 1953, pp. 3–8.